Table S1. Comparative performance of top-performing FDA-approved drugs as potential inhibitors of the RBD of SARS-CoV-2 variants.

Drug	DrugBank Database ID	Docking Score (%)					
		Wild	B.1.1.7	B.1.351	P.1	Mean	Std. Dev.
Carboprost tromethamine	DB00429	91.36	92.63	92.77	92.25	92.25	0.63
Bimatoprost	DB00905	91.51	92.26	92.14	93.10	92.25	0.65
Salmeterol	DB00938	92.94	92.17	91.98	91.89	92.25	0.48
Latanoprost	DB00654	92.08	92.50	91.07	92.72	92.09	0.73
Alprostadil	DB00770	90.88	92.37	92.15	92.46	91.97	0.73
Tafluprost	DB08819	91.60	92.28	91.77	92.12	91.94	0.31
Mupirocin	DB00410	90.92	91.25	92.94	92.55	91.92	0.98
Vilanterol	DB09082	92.63	91.65	91.82	91.52	91.91	0.50
Dinoprost	DB12789	91.18	92.00	91.92	92.45	91.89	0.53
Dinoprost tromethamine	DB01160	91.80	91.71	91.57	91.63	91.68	0.10
Dinoprostone	DB00917	90.45	92.02	92.01	92.13	91.65	0.80
Dopexamine	DB12313	91.80	91.74	90.64	92.09	91.57	0.64
Netarsudil	DB13931	92.64	90.80	91.40	91.24	91.52	0.79
Mirabegron	DB08893	92.08	91.74	91.05	91.18	91.51	0.48
Oxetacaine	DB12532	90.89	91.84	91.87	91.31	91.48	0.47
Zofenopril	DB13166	90.55	91.52	91.60	91.72	91.35	0.54
Treprostinil	DB00374	90.39	91.52	91.43	91.95	91.32	0.66
Silodosin	DB06207	91.81	90.46	91.51	91.49	91.32	0.59
Lisinopril	DB00722	90.35	92.18	91.06	91.67	91.32	0.79
Avapritinib	DB15233	91.56	91.08	91.25	91.35	91.31	0.20
Aclidinium	DB08897	90.44	91.57	92.02	90.99	91.26	0.69
Quinapril	DB00881	90.97	90.98	91.73	91.31	91.25	0.36
Vilazodone	DB06684	91.22	91.12	91.08	91.55	91.24	0.21
Propafenone	DB01182	91.21	91.13	91.13	91.20	91.17	0.04
Tirbanibulin	DB06137	90.77	91.21	91.34	91.30	91.16	0.26
Vibegron	DB14895	91.48	91.10	90.98	91.06	91.16	0.22
Eliglustat	DB09039	91.44	90.32	91.43	91.30	91.12	0.54
Labetalol	DB00598	91.22	91.37	90.81	91.04	91.11	0.24
Panobinostat	DB06603	90.58	90.85	91.71	91.17	91.08	0.49
Oxyphenonium	DB00219	90.49	91.15	91.40	91.19	91.06	0.39

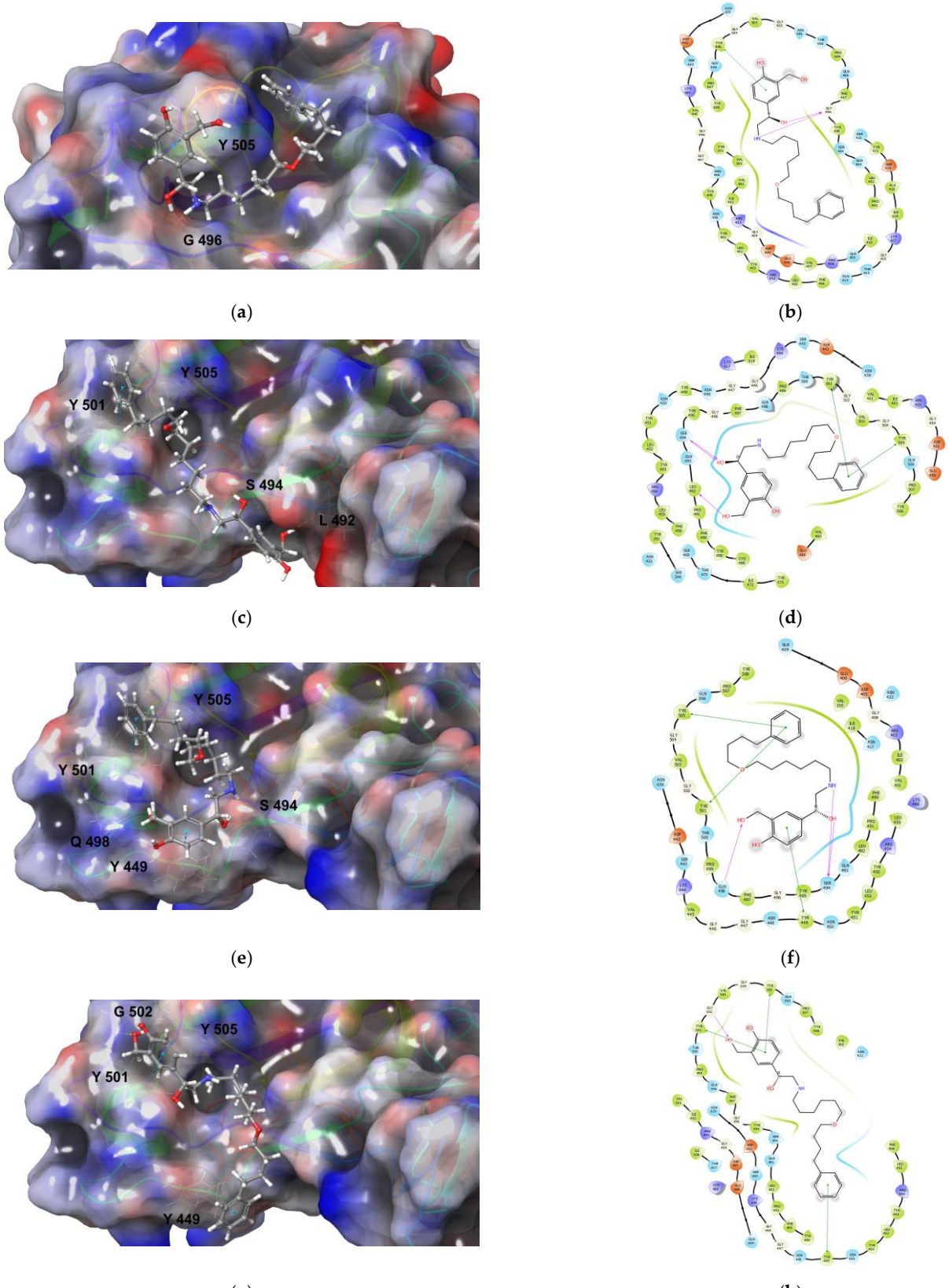

Figure S1. Structures of Salmeterol, the top-performing FDA-approved drug, docked in the RBD of SARS-CoV-2 and their corresponding ligand interaction diagrams: (**a–b**) Wild type; (**c–d**) B.1.1.7 variant; (**e–f**) B.1.351 variant; and (**g–h**) P.1 variant.

Table S2. ADMET properties of top-performing FDA-approved drugs as potential inhibitors of the RBD of SARS-CoV-2 variants (Green: excellent; Yellow: medium; Red: poor).

Drug	Physicochemical Properties						
	Molar Mass (g mol^{-1})	Topological-Polar Surface Area (A^3)	No. of Hydrogen Bond Donors	No. of Hydrogen Bond Acceptors	LogS (Solubility, mol/L)	LogP (Distribution Coefficient, mol/L)	$LogD_{7.4}$ (Distribution Coefficient, mol/L)
Carboprost tromethamine	368.26	97.99	5	4	−3.429	2.433	1.856
Bimatoprost	415.27	89.79	5	4	−3.968	1.873	2.398
Salmeterol	415.27	81.95	5	4	−2.920	3.052	3.040
Latanoprost	432.29	86.99	5	3	−4.722	3.483	3.466
Alprostadil	354.24	94.83	5	3	−3.755	3.072	1.992
Tafluprost	452.24	75.99	5	2	−4.693	3.744	4.028
Mupirocin	500.3	146.05	9	4	−3.155	2.744	1.620
Vilanterol	485.17	91.18	6	4	−3.633	3.009	3.040
Dinoprost	354.24	97.99	5	4	-3.607	2.200	1.630
Dinoprost tromethamine	354.24	97.99	5	4	−3.607	2.200	1.630
Dinoprostone	352.22	94.83	5	3	−3.819	1.844	0.970
Dopexamine	356.25	64.52	4	4	−2.406	2.542	3.117
Netarsudil	453.21	94.31	6	3	−3.866	4.311	3.433
Mirabegron	396.16	101	6	5	−2.888	1.183	1.209
Oxetacaine	467.31	64.09	6	1	−2.874	3.818	3.187
Zofenopril	429.11	74.68	5	1	−4.739	4.009	3.602
Treprostinil	390.24	86.99	5	3	−4.428	4.334	3.486
Silodosin	495.23	97.05	7	4	−4.951	3.368	3.084
Lisinopril	405.23	132.96	8	5	−1.702	−1.535	−0.435
Avapritinib	498.24	106.29	10	2	−4.261	3.642	2.473
Aclidinium	484.16	55.76	5	1	−1.118	4.030	2.506
Quinapril	438.22	95.94	7	2	−2.867	3.038	2.207
Vilazodone	441.22	102.29	7	3	−5.027	4.082	3.259
Propafenone	341.2	58.56	4	2	−4.058	3.423	3.384
Tirbanibulin	431.22	63.69	6	1	−3.944	2.982	3.015
Vibegron	444.22	96.25	7	3	−2.141	0.637	1.810
Eliglustat	404.27	71.03	6	2	−3.670	3.356	3.179
Labetalol	328.18	95.58	5	5	−3.213	2.358	1.898
Panobinostat	349.18	80.64	5	4	−3.557	2.727	1.828
Oxyphenonium	348.25	46.53	4	1	0.137	2.940	1.991

Drug	Absorption			Distribution			Excretion
	$LogP_{app}$ (Caco-2 Perme-ability)	$LogP_{app}$ (MDCK Perme-ability)	Plasma Protein Binding (%)	Volume Distribution (L/kg)	Blood-Brain Barrier (Probability)	% Unbound in Plasma	Clearance (mL/min/kg)
Carboprost tromethamine	−5.592	7.15×10^{-5}	87.859	0.389	0.026	7.055	4.598
Bimatoprost	−5.175	3.58×10^{-5}	88.984	0.678	0.043	3.488	6.573
Salmeterol	−5.024	2.93×10^{-5}	86.638	1.902	0.249	14.482	10.893
Latanoprost	−5.006	1.58×10^{-4}	95.468	0.978	0.035	2.545	9.674
Alprostadil	−5.306	3.63×10^{-5}	86.320	0.408	0.064	2.761	4.441
Tafluprost	−4.817	2.07×10^{-5}	99.519	0.911	0.031	1.487	5.745
Mupirocin	−5.436	4.15×10^{-5}	88.051	0.431	0.124	9.402	3.481
Vilanterol	−5.556	3.55×10^{-5}	90.476	1.657	0.188	5.704	7.424
Dinoprost	−5.604	5.20×10^{-5}	87.130	0.335	0.022	5.243	3.856
Dinoprost tromethamine	−5.604	5.20×10^{-5}	87.130	0.335	0.022	5.243	3.856
Dinoprostone	−5.476	4.62×10^{-5}	83.662	0.320	0.006	5.707	4.801

Dopexamine	−5.818	1.26×10^{-5}	73.172	1.241	0.208	34.185	14.033
Netarsudil	−5.273	8.79×10^{-6}	96.563	2.592	0.794	2.539	8.793
Mirabegron	−5.936	1.04×10^{-5}	55.901	2.485	0.489	49.057	6.503
Oxetacaine	−4.860	4.05×10^{-5}	78.662	0.814	0.393	24.293	10.163
Zofenopril	−5.430	1.32×10^{-5}	97.900	0.176	0.212	0.595	6.476
Treprostinil	−5.235	5.48×10^{-6}	96.155	0.257	0.087	4.004	11.490
Silodosin	−5.292	1.16×10^{-5}	75.921	2.633	0.056	9.936	5.471
Lisinopril	−6.194	8.06×10^{-5}	19.629	0.494	0.159	62.438	1.159
Avapritinib	−5.132	2.25×10^{-5}	91.676	2.532	0.387	11.821	8.594
Aclidinium	−5.167	7.14×10^{-5}	94.170	1.253	0.241	1.397	2.284
Quinapril	−5.791	3.65×10^{-5}	94.054	0.277	0.073	8.943	1.676
Vilazodone	−5.177	1.28×10^{-5}	95.880	2.424	0.573	6.176	6.247
Propafenone	−5.023	2.12×10^{-5}	89.554	1.836	0.365	6.210	12.604
Tirbanibulin	−4.715	2.38×10^{-5}	95.752	2.174	0.805	5.522	11.273
Vibegron	−5.430	6.12×10^{-6}	70.478	2.544	0.527	32.896	1.644
Eliglustat	−5.053	3.79×10^{-5}	81.864	1.806	0.738	11.390	6.663
Labetalol	−5.439	6.69×10^{-6}	74.952	4.114	0.101	43.445	13.381
Panobinostat	−5.283	6.00×10^{-6}	85.303	0.698	0.271	10.724	1.537
Oxyphenonium	−5.329	1.03×10^{-4}	84.090	0.822	0.154	13.468	9.649

Drug	Metabolism		Toxicity		
	Cytochrome 450 Inhibitor	Cytochrome 450 Substrate	hERG Blocker (Probability)	Human Hepatoxicity (Probability)	Ames Mutagenicity (Probability)
Carboprost tromethamine		CYP2C9	0.042	0.278	0.005
Bimatoprost		CYP2C19, CYP2C9	0.301	0.303	0.013
Salmeterol	CYP2D6		0.510	0.489	0.105
Latanoprost		CYP2C9	0.536	0.515	0.010
Alprostadil		CYP1A2, CYP2C19, CYP2C9	0.025	0.292	0.011
Tafluprost	CYP2C19, CYP2C9	CYP2C9	0.618	0.636	0.048
Mupirocin		CYP2C9	0.101	0.101	0.050
Vilanterol	CYP2D6, CYP3A4		0.519	0.712	0.090
Dinoprost		CYP2C9	0.045	0.312	0.008
Dinoprost tromethamine		CYP2C9	0.045	0.312	0.008
Dinoprostone		CYP1A2, CYP2C9	0.025	0.207	0.007
Dopexamine	CYP2D6	CYP2D6, CYP3A4	0.717	0.357	0.341
Netarsudil	CYP2C19, CYP2C9, CYP2D6, CYP3A4	CYP1A2, CYP2D6, CYP3A4	0.921	0.790	0.796
Mirabegron		CYP3A4	0.875	0.947	0.430
Oxetacaine	CYP2C19, CYP2D6, CYP3A4	CYP2C19, CYP3A4	0.049	0.097	0.009
Zofenopril		CYP2C9	0.032	0.872	0.004
Treprostinil		CYP2C9	0.149	0.311	0.007
Silodosin	CYP2D6	CYP2D6, CYP3A4	0.871	0.957	0.074
Lisinopril			0.036	0.977	0.004
Avapritinib	CYP2C19	CYP3A4	0.800	0.898	0.231
Aclidinium	CYP2D6	CYP2D6, CYP3A4	0.652	0.782	0.020
Quinapril			0.133	0.968	0.003
Vilazodone		CYP1A2, CYP2D6	0.987	0.943	0.418
Propafenone	CYP1A2, CYP2D6	CYP2C19, CYP2D6	0.920	0.582	0.215
Tirbanibulin	CYP2C19, CYP2C9, CYP2D6, CYP3A4	CYP2D6	0.925	0.497	0.178
Vibegron		CYP3A4	0.786	0.954	0.029
Eliglustat	CYP2D6, CYP3A4	CYP1A2, CYP2C19, CYP2D6, CYP3A4	0.940	0.059	0.019

Labetalol	CYP2D6	CYP2D6	0.592	0.478	0.018
Panobinostat		CYP2C9, CYP2D6	0.735	0.997	0.991
Oxyphenonium	CYP2D6		0.237	0.018	0.010

Drug	Toxicity		Drug-likeness			
	Carcinogenicity (Probability)	Respiratory Toxicity (Probability)	Drug-likeness Score	Synthetic Accessibility Score	MCE-18 Score	Natural Product-likeness Score
Carboprost tromethamine	0.050	0.861	0.312	4.140	24.973	1.887
Bimatoprost	0.028	0.678	0.312	3.871	42.333	1.012
Salmeterol	0.020	0.385	0.310	2.720	22.000	0.201
Latanoprost	0.114	0.337	0.247	3.855	45.256	1.176
Alprostadil	0.073	0.431	0.348	3.672	20.000	1.698
Tafluprost	0.115	0.917	0.274	4.008	52.103	0.580
Mupirocin	0.318	0.951	0.109	4.606	38.958	1.702
Vilanterol	0.034	0.148	0.259	2.980	26.000	−0.169
Dinoprost	0.067	0.844	0.319	3.979	20.571	1.936
Dinoprost tromethamine	0.067	0.844	0.319	3.979	20.571	1.936
Dinoprostone	0.184	0.431	0.370	3.874	20.118	2.028
Dopexamine	0.013	0.759	0.327	2.055	10.000	0.229
Netarsudil	0.078	0.830	0.389	2.768	46.000	−0.930
Mirabegron	0.034	0.719	0.359	3.014	32.000	−0.943
Oxetacaine	0.052	0.004	0.521	2.874	19.000	−0.482
Zofenopril	0.818	0.204	0.716	3.436	58.966	−0.378
Treprostinil	0.310	0.818	0.532	3.870	60.462	1.335
Silodosin	0.075	0.816	0.370	3.216	65.270	−0.832
Lisinopril	0.017	0.361	0.384	3.172	45.394	0.201
Avapritinib	0.957	0.451	0.394	3.455	107.000	−1.684
Aclidinium	0.031	0.939	0.273	4.216	91.216	−0.042
Quinapril	0.014	0.038	0.584	3.227	60.257	−0.319
Vilazodone	0.228	0.981	0.422	2.597	58.118	−1.199
Propafenone	0.103	0.138	0.487	2.389	22.000	−0.363
Tirbanibulin	0.072	0.164	0.563	2.112	42.471	−1.486
Vibegron	0.128	0.905	0.543	3.839	88.400	−0.249
Eliglustat	0.080	0.939	0.553	3.071	52.923	−0.220
Labetalol	0.028	0.517	0.597	2.809	26.000	−0.207
Panobinostat	0.956	0.912	0.170	2.536	16.000	−0.527
Oxyphenonium	0.016	0.884	0.578	3.116	50.143	0.087

Table S3. Comparative performance of top-performing investigational drugs as potential inhibitors of the RBD of SARS-CoV-2 variants.

DrugBank Database ID	Docking Score (%)					
	Wild	**B.1.1.7**	**B.1.351**	**P.1**	**Mean**	**Std. Dev.**
DB15106	91.99	92.90	92.65	92.86	92.60	0.42
DB12100	92.42	92.42	91.99	91.59	92.11	0.40
DB12133	91.84	92.90	92.24	91.26	92.06	0.69
DB11858	91.18	92.99	92.01	91.58	91.94	0.78
DB12511	91.17	91.51	92.39	92.20	91.82	0.57
DB15321	92.05	91.33	91.89	91.96	91.81	0.32
DB12259	90.76	91.82	92.82	91.56	91.74	0.85
DB16315	91.67	91.70	91.68	91.71	91.69	0.02
DB12708	91.43	92.46	91.49	91.26	91.66	0.54
DB12013	91.56	91.31	91.82	91.73	91.61	0.22
DB12022	89.96	91.99	92.14	92.29	91.60	1.10
DB11818	91.25	91.59	91.60	91.73	91.54	0.21
DB15410	90.79	91.89	91.74	91.56	91.50	0.49
DB11781	90.24	91.96	91.98	91.75	91.48	0.83
DB05104	90.19	92.03	91.97	91.70	91.47	0.87
DB05562	91.13	91.54	91.64	91.56	91.47	0.23
DB12961	91.45	91.37	90.97	91.92	91.43	0.39
DB12109	90.58	92.23	91.45	91.35	91.40	0.67
DB15048	91.47	91.06	91.46	91.61	91.40	0.24
DB12408	90.57	91.39	91.73	91.90	91.40	0.59
DB12985	90.74	91.62	90.40	92.83	91.40	1.08
DB13312	91.28	91.07	91.63	91.59	91.39	0.27
DB02056	91.33	91.52	91.39	91.15	91.35	0.15
DB12043	90.69	91.61	91.72	91.37	91.35	0.46
DB12848	90.48	91.42	91.68	91.70	91.32	0.57
DB05713	91.49	91.11	91.45	91.17	91.31	0.19
DB09211	90.93	91.40	91.31	91.57	91.30	0.27
DB15419	91.21	91.47	90.31	92.19	91.30	0.78
DB05590	90.63	91.29	91.59	91.65	91.29	0.47
DB15212	91.70	90.71	91.27	91.43	91.28	0.42

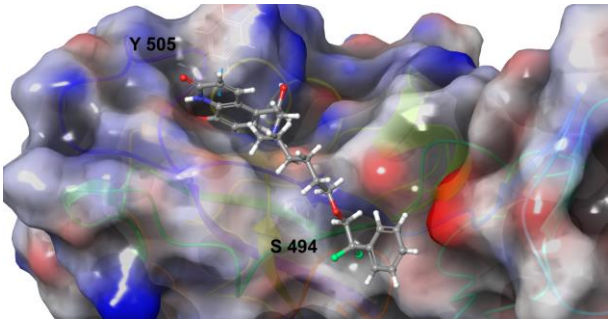

(**a**)

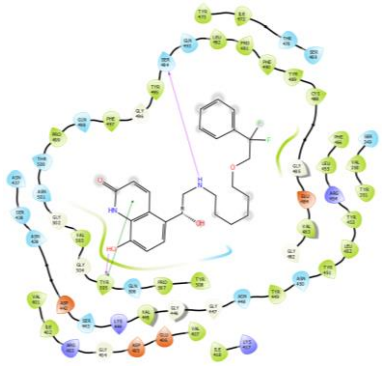

(**b**)

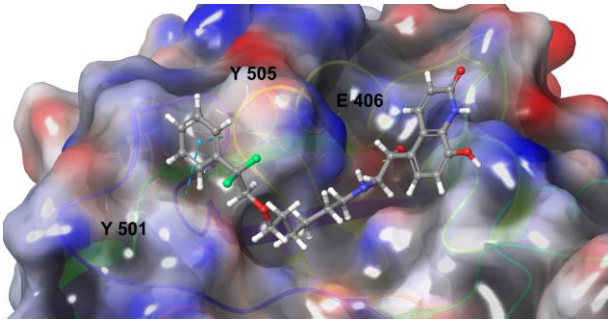

(**c**)

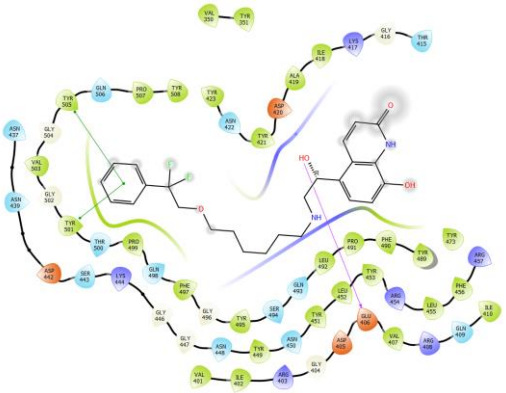

(**d**)

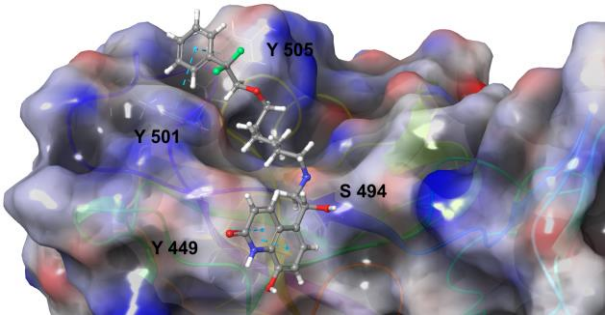

(**e**)

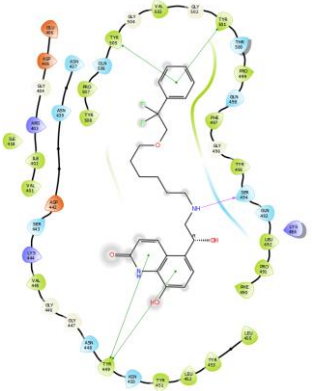

(**f**)

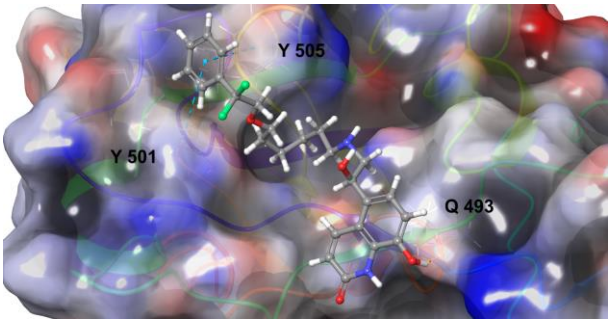

(**g**)

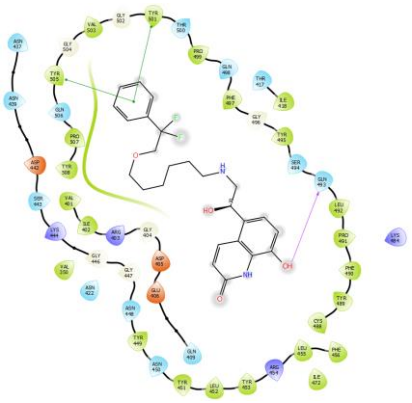

(**h**)

Figure S2. Structures of Abediterol, the top-performing investigational drug, docked in the RBD of SARS-CoV-2 and their corresponding ligand interaction diagrams: (**a–b**) Wild type; (**c–d**) B.1.1.7 variant; (**e–f**) B.1.351 variant; and (**g–h**) P.1 variant.

Table S4. ADMET properties of top-performing investigational drugs as potential inhibitors of the RBD of SARS-CoV-2 variants (Green: excellent; Yellow: medium; Red: poor).

DrugBank Database ID	Physicochemical Properties						
	Molar Mass (g mol^{-1})	Topological-Polar Surface Area (A^3)	No. of Hydrogen Bond Donors	No. of Hydrogen Bond Acceptors	LogS (Solubility, mol/L)	LogP (Distribution Coefficient, mol/L)	$LogD_{7.4}$ (Distribution Coefficient, mol/L)
DB15106	480.19	115.47	9	3	−3.481	3.233	2.979
DB12100	460.22	94.58	6	4	−4.279	3.475	3.192
DB12133	376.22	97.99	5	4	−3.880	3.065	1.530
DB11858	496.26	149.95	8	6	−3.002	−0.501	−0.092
DB12511	470.18	94.15	7	1	−5.191	5.035	5.032
DB15321	495.27	120.25	8	4	−3.699	4.113	3.364
DB12259	427.25	94.39	7	3	−3.399	3.083	2.583
DB16315	450.21	93.06	6	2	−4.121	1.909	2.296
DB12708	465.18	130	8	3	−3.377	0.366	−0.647
DB12013	457.29	107.1	7	4	−2.906	2.648	1.858
DB12022	468.17	96.8	7	1	−4.282	4.022	2.957
DB11818	494.25	104.98	9	1	−3.665	2.704	2.618
DB15410	341.2	58.56	4	2	−4.032	3.433	3.472
DB11781	406.21	128.45	8	4	−3.209	2.767	2.060
DB05104	414.23	43.78	4	1	−3.628	3.849	3.472
DB05562	450.27	81.75	7	2	−3.389	3.349	3.210
DB12961	336.23	77.76	4	3	−3.537	2.254	0.805
DB12109	388.15	37.3	2	1	−5.073	4.813	4.646
DB15048	416.18	108.61	7	4	−4.358	2.311	2.169
DB12408	444.24	75.79	5	3	−3.571	3.621	3.132
DB12985	394.21	98.8	8	3	−2.741	2.076	1.842
DB13312	452.23	95.94	7	2	−3.163	3.093	2.756
DB02056	352.22	94.83	5	3	−3.281	2.213	1.132
DB12043	482.25	85.22	6	2	−5.075	4.211	4.144
DB12848	372.14	107.43	9	1	−2.192	1.541	1.754
DB05713	459.26	71.68	7	2	−2.440	2.573	2.483
DB09211	380.26	94.83	5	3	−4.011	3.558	2.412
DB15419	394.16	106.76	8	3	−3.808	1.239	1.559
DB05590	428.23	102.26	7	4	−2.800	0.363	1.238
DB15212	490.21	94.26	8	1	−5.188	5.188	3.730

DrugBank Database ID	Absorption		Distribution				Excretion
	$LogP_{app}$ (Caco-2 Permeability)	$LogP_{app}$ (MDCK Permeability)	Plasma Protein Binding (%)	Volume Distribution (L/kg)	Blood-Brain Barrier (Probability)	% Unbound in Plasma	Clearance (mL/min/kg)
DB15106	−6.101	3.71×10^{-6}	72.754	2.918	0.535	32.044	5.312
DB12100	−5.897	2.36×10^{-5}	89.836	2.122	0.214	8.761	5.83
DB12133	−5.157	1.05×10^{-5}	95.185	0.472	0.300	1.481	3.578
DB11858	−5.575	3.96×10^{-6}	85.822	0.243	0.005	8.502	2.25
DB12511	−4.635	1.67×10^{-5}	101.019	0.384	0.026	0.897	0.473
DB15321	−5.423	4.11×10^{-5}	81.392	0.595	0.455	6.880	1.203
DB12259	−5.090	2.53×10^{-5}	59.020	2.25	0.626	34.637	6.053
DB16315	−4.800	1.63×10^{-5}	67.474	0.517	0.796	25.365	8.26
DB12708	−5.726	8.65×10^{-6}	84.458	0.286	0.005	4.689	2.058
DB12013	−5.509	5.50×10^{-5}	80.282	1.332	0.220	22.992	3.538
DB12022	−5.851	4.20×10^{-5}	98.983	0.376	0.006	1.174	6.517
DB11818	−5.237	1.87×10^{-5}	87.289	1.788	0.055	8.656	6.938
DB15410	−4.872	2.14×10^{-5}	89.613	2.091	0.289	6.625	12.451
DB11781	−5.311	1.00×10^{-4}	81.712	0.789	0.499	15.970	1.134

DB05104	−4.962	2.55×10^{-5}	92.658	3.569	0.596	4.579	9.584
DB05562	−5.549	3.63×10^{-5}	62.777	1.442	0.968	43.707	3.715
DB12961	−5.195	7.57×10^{-5}	88.249	0.235	0.042	9.047	5.686
DB12109	−4.987	1.33×10^{-5}	99.398	0.606	0.095	0.407	7.253
DB15048	−5.148	5.85×10^{-6}	96.521	0.73	0.114	2.532	9.541
DB12408	−4.930	1.78×10^{-5}	94.108	2.915	0.905	4.696	10.171
DB12985	−5.385	2.25×10^{-6}	86.444	1.801	0.945	8.508	3.574
DB13312	−5.534	3.99×10^{-5}	94.314	0.139	0.049	6.154	1.89
DB02056	−5.315	2.92×10^{-5}	89.316	0.27	0.320	11.181	8.95
DB12043	−4.892	4.05×10^{-5}	93.940	0.638	0.039	2.037	6.077
DB12848	−4.743	2.58×10^{-5}	88.633	1.921	0.537	15.274	9.314
DB05713	−5.635	5.41×10^{-6}	75.983	2.17	0.968	43.943	4.047
DB09211	−5.055	2.69×10^{-5}	93.461	0.389	0.137	2.817	7.267
DB15419	−4.996	1.26×10^{-5}	89.928	1.742	0.616	5.768	1.133
DB05590	−5.714	4.56×10^{-6}	45.643	1.91	0.799	55.357	11.93
DB15212	−4.927	1.85×10^{-5}	102.226	0.412	0.040	1.053	4.445

DrugBank Database ID	Metabolism		Toxicity		
	Cytochrome 450 Inhibitor	Cytochrome 450 Substrate	hERG Blocker (Probability)	Human Hepatoxicity (Probability)	Ames Mutagenicity (Probability)
DB15106	CYP3A4	CYP1A2, CYP3A4	0.883	0.988	0.142
DB12100	CYP2D6, CYP3A4		0.786	0.835	0.672
DB12133		CYP2C9, CYP2D6	0.070	0.859	0.009
DB11858		CYP2C9	0.143	0.372	0.034
DB12511	CYP2C19, CYP2C9	CYP2C9	0.267	0.858	0.096
DB15321	CYP2C9, CYP3A4	CYP2C9	0.126	0.993	0.134
DB12259		CYP2D6	0.296	0.987	0.983
DB16315		CYP2C19, CYP3A4	0.087	0.421	0.016
DB12708		CYP2C19, CYP2C9, CYP3A4	0.074	0.354	0.010
DB12013	CYP2D6		0.636	0.989	0.004
DB12022	CYP2C19, CYP2C9, CYP3A4	CYP2C9, CYP3A4	0.206	0.371	0.004
DB11818	CYP3A4	CYP3A4	0.028	0.784	0.008
DB15410	CYP1A2, CYP2D6, CYP3A4	CYP2D6	0.925	0.471	0.085
DB11781		CYP2C9	0.025	0.985	0.025
DB05104	CYP2D6	CYP2C19, CYP3A4	0.382	0.658	0.020
DB05562	CYP3A4	CYP2C19, CYP2D6, CYP3A4	0.830	0.775	0.025
DB12961		CYP2C9, CYP2D6	0.065	0.861	0.033
DB12109			0.042	0.073	0.005
DB15048		CYP2D6	0.301	0.248	0.242
DB12408	CYP2D6	CYP2C19, CYP3A4	0.779	0.232	0.258
DB12985			0.685	0.996	0.875
DB13312	CYP2C19		0.444	0.969	0.003
DB02056		CYP2C9	0.019	0.224	0.009
DB12043	CYP2C9	CYP2C9	0.432	0.505	0.030
DB12848	CYP1A2		0.072	0.924	0.332
DB05713		CYP2C19, CYP2D6	0.615	0.450	0.015
DB09211		CYP2C9	0.019	0.212	0.009
DB15419			0.840	0.997	0.513
DB05590		CYP2D6	0.250	0.821	0.163
DB15212	CYP2C19, CYP2C9, CYP2D6	CYP1A2, CYP2C9, CYP2D6	0.702	0.925	0.008

Toxicity	Drug-likeness

DrugBank Database ID	Carcino-genicity (Probability)	Respiratory Toxicity (Probability)	Drug-likeness Score	Synthetic Accessi-bility Score	MCE-18 Score	Natural Product-likeness Score
DB15106	0.116	0.958	0.34	3.191	24.000	−1.57
DB12100	0.066	0.948	0.287	3.152	38.000	−0.091
DB12133	0.058	0.326	0.394	3.632	18.000	1.42
DB11858	0.326	0.629	0.098	4.169	6.000	1.484
DB12511	0.538	0.038	0.213	2.415	21.000	−0.925
DB15321	0.205	0.556	0.067	3.029	55.146	−0.604
DB12259	0.706	0.869	0.112	2.793	13.000	−0.297
DB16315	0.069	0.046	0.271	3.934	44.947	0.739
DB12708	0.023	0.014	0.317	3.938	51.765	0.797
DB12013	0.037	0.874	0.527	4.538	82.591	−0.435
DB12022	0.128	0.014	0.505	2.286	22.000	−1.579
DB11818	0.504	0.041	0.659	4.208	99.429	−0.107
DB15410	0.080	0.363	0.487	2.389	22.000	−0.363
DB11781	0.059	0.849	0.117	3.914	49.545	0.166
DB05104	0.076	0.927	0.633	2.953	67.800	−0.537
DB05562	0.081	0.925	0.536	2.336	45.231	−1.615
DB12961	0.527	0.884	0.253	3.709	3.000	1.888
DB12109	0.502	0.015	0.411	2.694	20.000	−0.348
DB15048	0.150	0.007	0.579	3.728	78.471	1.045
DB12408	0.439	0.938	0.51	2.672	54.054	−0.047
DB12985	0.908	0.892	0.257	2.782	49.241	−1.122
DB13312	0.023	0.041	0.509	3.194	60.081	−0.265
DB02056	0.188	0.225	0.37	3.966	20.118	1.924
DB12043	0.039	0.828	0.385	4.282	68.372	0.363
DB12848	0.951	0.649	0.5	2.697	24.000	−2.003
DB05713	0.035	0.985	0.616	2.906	90.316	−1.115
DB09211	0.668	0.522	0.333	4.247	22.105	2.049
DB15419	0.856	0.627	0.263	3.91	88.000	−1.127
DB05590	0.152	0.163	0.484	3.318	61.343	−0.237
DB15212	0.365	0.152	0.244	2.917	44.000	−0.853

Table S5. Comparative performance of top-performing experimental drugs as potential inhibitors of the RBD of SARS-CoV-2 variants.

DrugBank Database ID	Docking Score (%)					
	Wild	**B.1.1.7**	**B.1.351**	**P.1**	**Mean**	**Std. Dev.**
DB03438	92.27	92.70	92.44	92.14	92.39	0.24
DB01871	92.03	92.35	93.13	92.01	92.38	0.52
DB14067	92.71	92.44	92.44	91.55	92.29	0.51
DB06835	91.22	92.71	92.75	91.70	92.10	0.76
DB07136	91.98	91.97	92.53	91.59	92.02	0.39
DB08420	92.41	92.19	91.34	92.00	91.99	0.46
DB04136	90.97	92.48	92.17	92.24	91.97	0.68
DB07521	91.58	92.06	92.02	92.05	91.93	0.23
DB03949	91.16	92.00	92.42	92.11	91.92	0.54
DB08180	92.03	91.82	91.45	92.36	91.92	0.38
DB07349	92.11	91.55	92.61	91.36	91.91	0.57
DB07589	91.53	92.20	91.48	92.34	91.89	0.45
DB07219	91.20	92.07	91.81	92.45	91.88	0.53
DB03565	91.09	92.36	92.03	91.84	91.83	0.54
DB01834	91.19	91.55	91.80	92.70	91.81	0.64
DB03866	91.19	92.15	91.60	92.05	91.75	0.44
DB04244	91.11	92.31	92.12	91.36	91.73	0.58
DB07157	91.28	92.04	92.34	91.22	91.72	0.56
DB02307	91.01	92.21	92.06	91.48	91.69	0.55
DB07269	90.49	92.10	92.14	92.02	91.69	0.80
DB08732	92.25	91.52	90.86	91.95	91.65	0.60
DB13203	90.59	92.08	91.84	92.07	91.65	0.71
DB08585	91.05	91.88	91.54	92.09	91.64	0.45
DB02112	91.41	91.70	91.64	91.80	91.64	0.17
DB04732	90.95	91.89	91.77	91.80	91.60	0.44
DB07841	90.96	92.18	91.48	91.79	91.60	0.52
DB02128	91.03	91.68	91.79	91.77	91.57	0.36
DB04118	91.17	90.98	92.04	92.01	91.55	0.55
DB06886	91.32	91.44	91.81	91.61	91.55	0.21
DB11425	91.99	91.74	91.15	91.30	91.55	0.39
DB07400	90.81	91.52	92.06	91.79	91.55	0.54

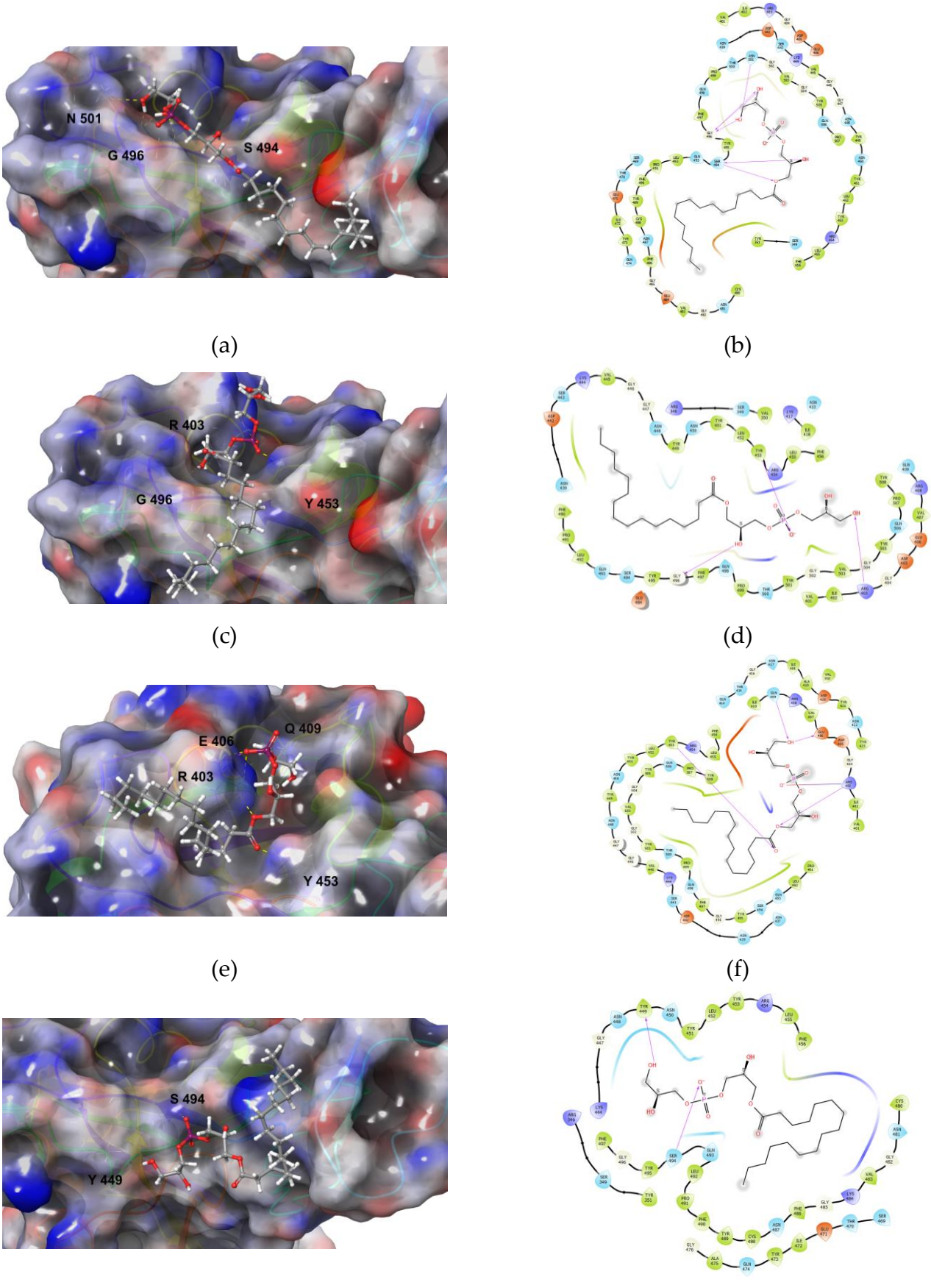

Figure S3. Structures of Lysophosphatidylglycerol, the top-performing experimental drug, docked in the RBD of SARS-CoV-2 and their corresponding ligand interaction diagrams: (a-b) Wild type; (c-d) B.1.1.7 variant; (e-f) B.1.351 variant; and (g-h) P.1 variant.

Table S6. ADMET properties of top-performing experimental drugs as potential inhibitors of the RBD of SARS-CoV-2 variants (Green: excellent; Yellow: medium; Red: poor).

	Physicochemical Properties						
DrugBank Database ID	Molar Mass (g mol^{-1})	Topological-Polar Surface Area (A^3)	No. of Hydrogen Bond Donors	No. of Hydrogen Bond Acceptors	LogS (Solubility, mol/L)	LogP (Distribution Coefficient, mol/L)	$LogD_{7.4}$ (Distribution Coefficient, mol/L)
DB03438	484.28	139.59	9	3	−3.456	3.700	2.105
DB01871	460.2	104.73	7	3	−4.187	3.230	3.132
DB14067	481.24	65.9	6	1	−4.134	3.965	3.690
DB06835	482.16	143.63	8	4	−1.126	−0.138	0.224
DB07136	496.18	143.63	8	4	−1.287	0.087	0.585
DB08420	434.21	139.68	8	5	−1.630	0.314	1.258
DB04136	485.28	165.61	10	5	−2.636	1.211	1.011
DB07521	483.16	68.43	6	4	−1.598	3.128	2.883
DB03949	492.17	115.73	7	4	−3.658	3.082	2.954
DB08180	453.2	110.21	8	1	−2.907	0.781	0.629
DB07349	456.21	145.66	10	2	−2.704	2.453	0.815
DB07589	485.16	121.52	7	5	−2.582	0.530	1.657
DB07219	473.25	117.34	9	2	−3.636	2.675	2.405
DB03565	489.26	131.22	9	2	−2.325	2.356	1.328
DB01834	501.16	179.05	10	7	−3.531	−2.040	−0.311
DB03866	368.22	85.22	6	2	−3.570	3.405	3.011
DB04244	481.2	108.39	7	3	−4.886	3.873	3.415
DB07157	450.16	145.02	9	4	−2.174	0.516	0.798
DB02307	441.19	158.82	9	6	−2.137	-0.348	0.258
DB07269	448.18	135.79	8	4	−1.666	1.055	1.017
DB08732	398.18	104.73	7	3	−2.944	2.054	2.075
DB13203	385.21	85.29	8	1	−1.213	1.154	1.181
DB08585	456.17	159.1	10	4	−1.892	−0.141	−0.128
DB02112	489.25	91.12	6	4	−4.212	4.127	2.814
DB04732	441.24	111.13	8	4	−3.171	1.823	3.329
DB07841	450.19	106.97	7	1	−2.593	4.273	1.271
DB02128	475.21	117.62	8	3	−3.345	2.532	2.486
DB04118	491.18	94.72	7	2	−4.608	4.170	3.855
DB06886	467.24	107.97	8	3	−3.543	2.850	2.834
DB11425	444.14	107.22	6	4	−3.779	2.790	2.093

	Absorption			Distribution			Excretion
DrugBank Database ID	$LogP_{app}$ (Caco-2 Permeability)	$LogP_{app}$ (MDCK Permeability)	Plasma Protein Binding (%)	Volume Distribution (L/kg)	Blood-Brain Barrier (Probability)	% Unbound in Plasma	Clearance (mL/min/kg)
DB03438	-5.157	4.56E-05	95.364	0.667	0.106	2.481	1.643
DB01871	-5.101	1.80E-04	96.207	0.536	0.061	5.004	7.029
DB14067	-5.519	2.03E-05	95.842	2.016	0.805	1.856	6.7
DB06835	-6.093	9.81E-06	34.018	0.429	0.071	59.888	0.969
DB07136	-6.028	9.76E-06	35.513	0.433	0.068	55.745	0.958
DB08420	-5.808	6.98E-06	85.854	0.843	0.118	15.493	4.925
DB04136	-5.631	5.52E-05	91.717	0.546	0.196	6.886	0.947
DB07521	-5.912	5.99E-06	60.971	1.028	0.149	58.314	4.669
DB03949	-6.177	5.05E-06	98.525	0.378	0.009	0.862	3.02
DB08180	-5.502	4.84E-05	74.231	0.884	0.975	10.472	1.757
DB07349	-5.074	9.44E-05	84.358	0.532	0.212	15.690	2.116
DB07589	-5.909	1.34E-05	44.369	0.709	0.034	37.404	3.822
DB07219	-5.158	4.86E-05	86.736	0.596	0.192	12.523	5.886
DB03565	-5.517	3.95E-05	86.335	0.797	0.101	5.811	1.175

DB01834	-6.631	5.30E-06	75.609	0.175	0.107	36.199	1.624
DB03866	-5.301	4.17E-05	95.943	0.408	0.005	2.422	2.072
DB04244	-5.808	1.53E-05	95.529	1.004	0.099	3.197	1.619
DB07157	-5.840	3.63E-05	41.008	0.453	0.156	53.543	1.262
DB02307	-6.291	6.60E-05	89.443	0.346	0.056	19.346	0.978
DB07269	-5.686	1.70E-05	33.189	0.666	0.199	58.990	1.073
DB08732	-5.038	1.21E-04	87.004	0.381	0.204	15.615	6.679
DB13203	-5.005	1.59E-05	66.213	1.698	0.888	35.397	2.337
DB08585	-5.405	4.93E-06	47.271	0.477	0.475	64.365	2.002
DB02112	-5.980	5.81E-06	90.550	1.069	0.802	3.646	0.97
DB04732	-5.601	2.87E-05	94.377	0.511	0.586	3.169	4.203
DB07841	-5.120	1.41E-05	84.889	4.663	0.102	4.477	1.775
DB02128	-4.979	7.70E-05	91.243	0.799	0.121	9.854	6.23
DB04118	-4.965	2.27E-05	96.536	0.839	0.077	2.005	5.099
DB06886	-5.337	1.32E-04	92.642	0.627	0.073	9.046	5.759
DB11425	-5.626	4.82E-06	98.154	0.331	0.110	1.694	7.333

DrugBank Database ID	Metabolism		Toxicity		
	Cytochrome 450 Inhibitor	Cytochrome 450 Substrate	hERG Blocker (Probability)	Human Hepatox-icity (Probability)	Ames Mutagenicity (Probability)
DB03438			0.347	0.029	0.016
DB01871	CYP2C19, CYP2C9, CYP2D6, CYP3A4		0.383	0.624	0.458
DB14067	CYP2C19, CYP2D6, CYP3A4	CYP2C19, CYP2D6, CYP3A4	0.986	0.701	0.049
DB06835		CYP2C9	0.016	0.690	0.007
DB07136		CYP2C9	0.020	0.706	0.006
DB08420		CYP2C9	0.212	0.988	0.044
DB04136		CYP2C9	0.183	0.187	0.444
DB07521	CYP2D6	CYP2C19	0.423	0.999	0.921
DB03949	CYP2C9	CYP2C9	0.124	0.635	0.037
DB08180		CYP2C9	0.020	0.511	0.003
DB07349			0.047	0.091	0.182
DB07589	CYP2C9, CYP3A4	CYP3A4	0.041	0.923	0.057
DB07219			0.020	0.506	0.015
DB03565			0.232	0.126	0.547
DB01834		CYP2C9	0.084	0.244	0.009
DB03866		CYP1A2, CYP2C19, CYP2C9, CYP2D6	0.108	0.326	0.848
DB04244	CYP2C19, CYP2C9, CYP3A4		0.444	0.836	0.007
DB07157		CYP2C9	0.031	0.253	0.009
DB02307		CYP2C9	0.031	0.735	0.006
DB07269		CYP2C9	0.029	0.261	0.012
DB08732			0.141	0.530	0.067
DB13203		CYP2C19, CYP3A4	0.186	0.086	0.094
DB08585		CYP2C9	0.006	0.042	0.037
DB02112		CYP1A2, CYP2D6	0.935	0.990	0.339
DB04732		CYP2C9	0.012	0.984	0.068
DB07841		CYP2C9	0.006	0.867	0.005
DB02128	CYP2C19, CYP2C9, CYP3A4		0.462	0.551	0.120
DB04118	CYP2C19, CYP2C9, CYP2D6, CYP3A4	CYP2C9, CYP3A4	0.640	0.573	0.915
DB06886	CYP2C19, CYP2C9, CYP3A4		0.069	0.906	0.009
DB11425		CYP2C9	0.206	0.461	0.009

DrugBank Database ID	Toxicity		Drug-likeness			
	Carcinogenicity (Probability)	Respiratory Toxicity (Probability)	Drug-likeness Score	Synthetic Accessibility Score	MCE-18 Score	Natural Product-likeness Score
DB03438	0.550	0.420	0.111	3.995	6.000	0.552
DB01871	0.217	0.015	0.408	2.765	34.000	0.027
DB14067	0.144	0.975	0.413	2.731	80.263	−1.029
DB06835	0.042	0.125	0.395	3.973	38.000	−0.3
DB07136	0.037	0.156	0.361	3.968	38.000	−0.279
DB08420	0.909	0.487	0.437	3.47	61.903	−0.668
DB04136	0.494	0.819	0.096	4.374	7.000	0.484
DB07521	0.054	0.827	0.25	4.277	72.600	−0.664
DB03949	0.122	0.021	0.264	3.109	38.000	0.091
DB08180	0.502	0.608	0.263	4.429	0.000	0.667
DB07349	0.761	0.081	0.169	4.089	7.000	0.718
DB07589	0.209	0.950	0.409	3.524	76.645	−0.588
DB07219	0.024	0.010	0.372	3.65	66.000	−0.387
DB03565	0.667	0.378	0.149	4.658	7.000	0.195
DB01834	0.018	0.035	0.262	3.767	65.625	0.545
DB03866	0.396	0.941	0.215	5.217	27.429	2.296
DB04244	0.213	0.418	0.389	3.221	40.000	−0.731
DB07157	0.011	0.037	0.466	3.873	34.000	−0.098
DB02307	0.070	0.033	0.306	3.067	30.000	0.175
DB07269	0.017	0.102	0.472	3.85	34.000	−0.045
DB08732	0.044	0.013	0.568	2.801	26.000	−0.014
DB13203	0.074	0.424	0.604	2.46	19.000	−1.471
DB08585	0.007	0.091	0.209	3.94	10.000	-0.255
DB02112	0.685	0.674	0.205	2.678	72.421	-0.319
DB04732	0.933	0.036	0.462	3.257	61.471	-0.792
DB07841	0.919	0.760	0.232	4.428	0.000	1.002
DB02128	0.048	0.020	0.371	2.968	34.000	−0.097
DB04118	0.868	0.706	0.304	3.876	101.486	0.243
DB06886	0.023	0.012	0.525	3.296	61.108	−0.39
DB11425	0.264	0.691	0.290	4.037	46.242	0.429

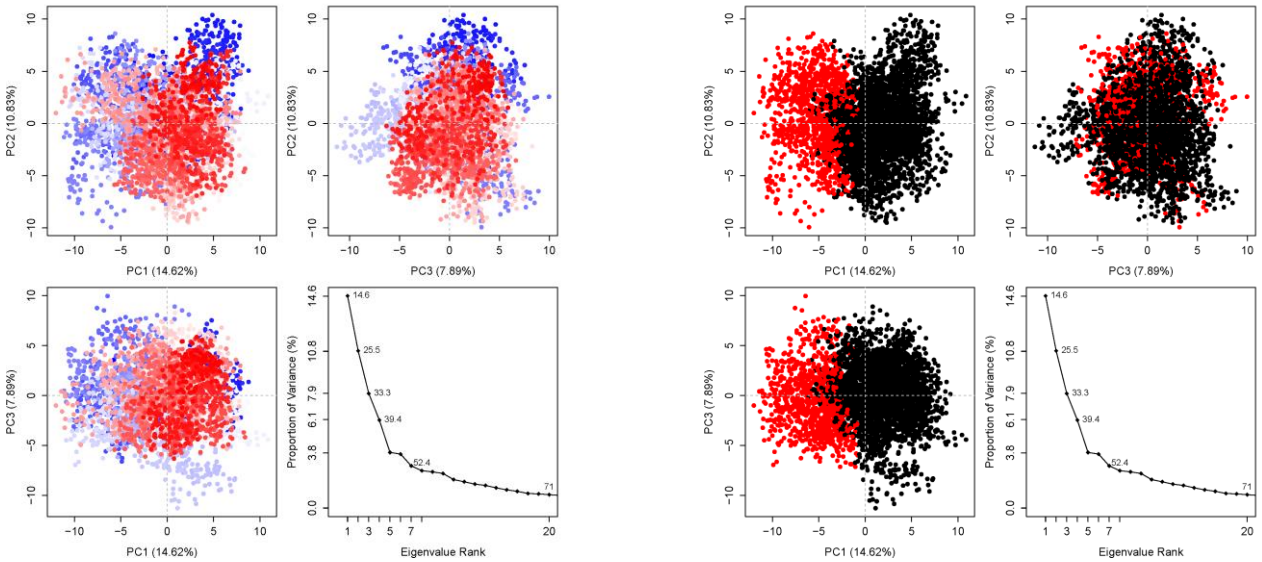

(**a**) (**b**)

Figure S4. (**a**) Principal Component Analysis (PCA) for the MD trajectory of Salmeterol binding into Wild-type RBD. The trajectory frames are colored from blue to white to red in time order. (**b**) Simple clustering in PC subspace. The conformations were divided into two clusters (black and red) according to the top 3 PC-spaces shown in the PC subspace.

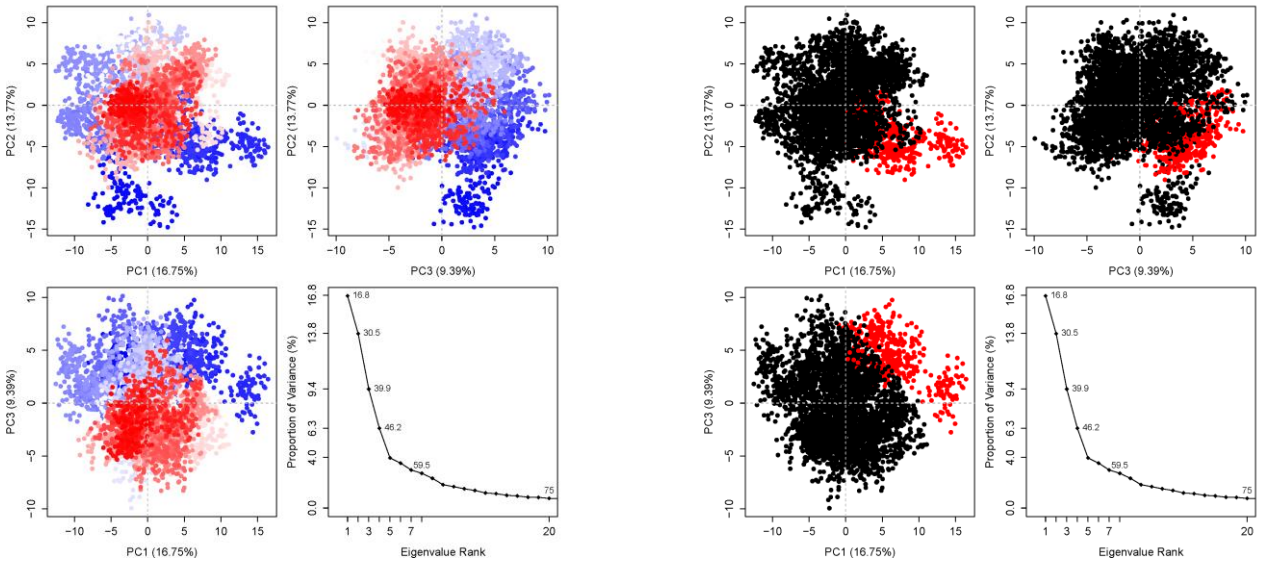

(**a**) (**b**)

Figure S5. (**a**) Principal Component Analysis (PCA) for the MD trajectory of the unbinding process between Salmeterol and Wild-type RBD. The trajectory frames are colored from blue to white to red in time order. (**b**) Simple clustering in PC subspace. The conformations were divided into two clusters (black and red) according to the top 3 PC-spaces shown in the PC subspace.

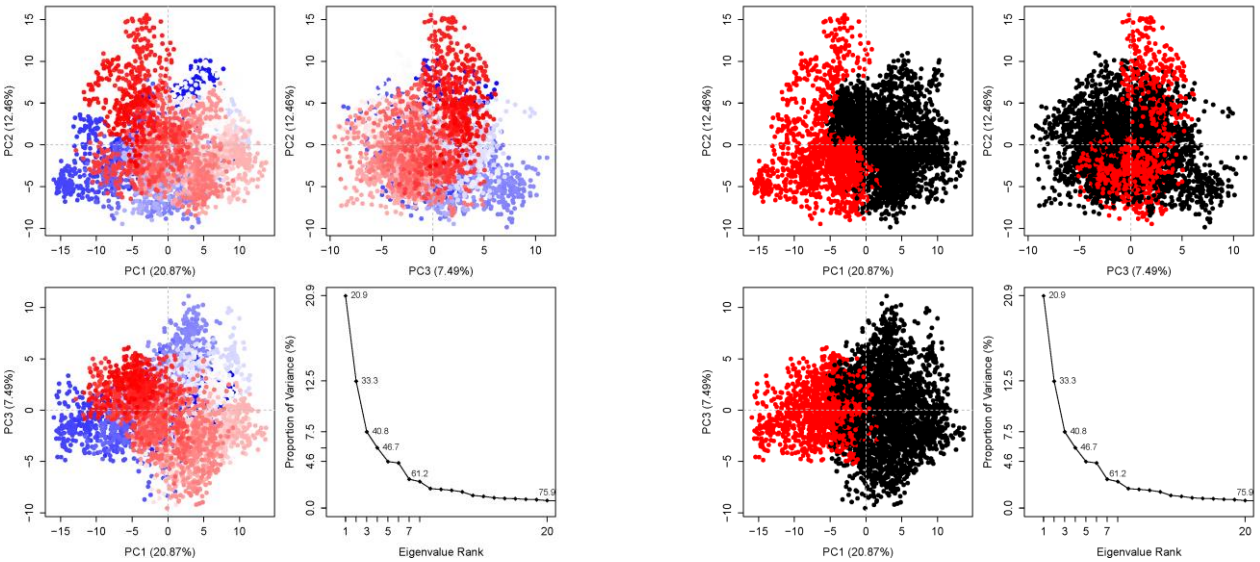

(a) (b)

Figure S6. (**a**) Principal Component Analysis (PCA) for the MD trajectory of Salmeterol binding into SARS-CoV-2 B.1.1.7 Variant RBD. The trajectory frames are colored from blue to white to red in time order. (**b**) Simple clustering in PC subspace. The conformations were divided into two clusters (black and red) according to the top 3 PC-spaces shown in the PC subspace.

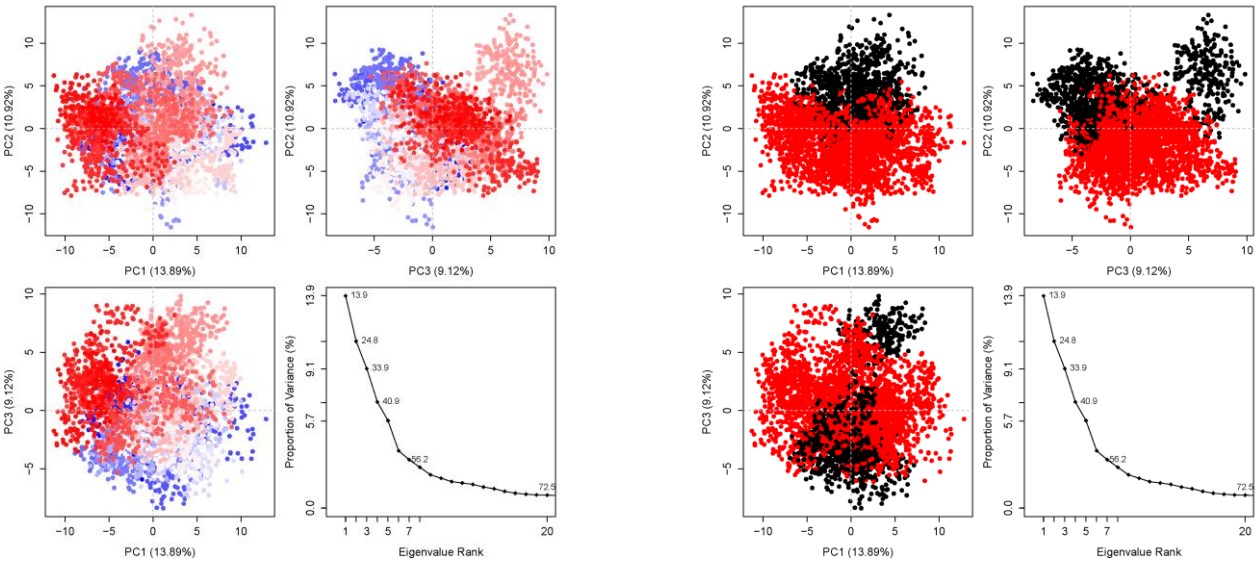

(**a**) (**b**)

Figure S7. (**a**) Principal Component Analysis (PCA) for the MD trajectory of the unbinding process between Salmeterol and SARS-CoV-2 B.1.1.7 RBD. The trajectory frames are colored from blue to white to red in time order. (**b**) Simple clustering in PC subspace. The conformations were divided into two clusters (black and red) according to the top 3 PC-spaces shown in the PC subspace.

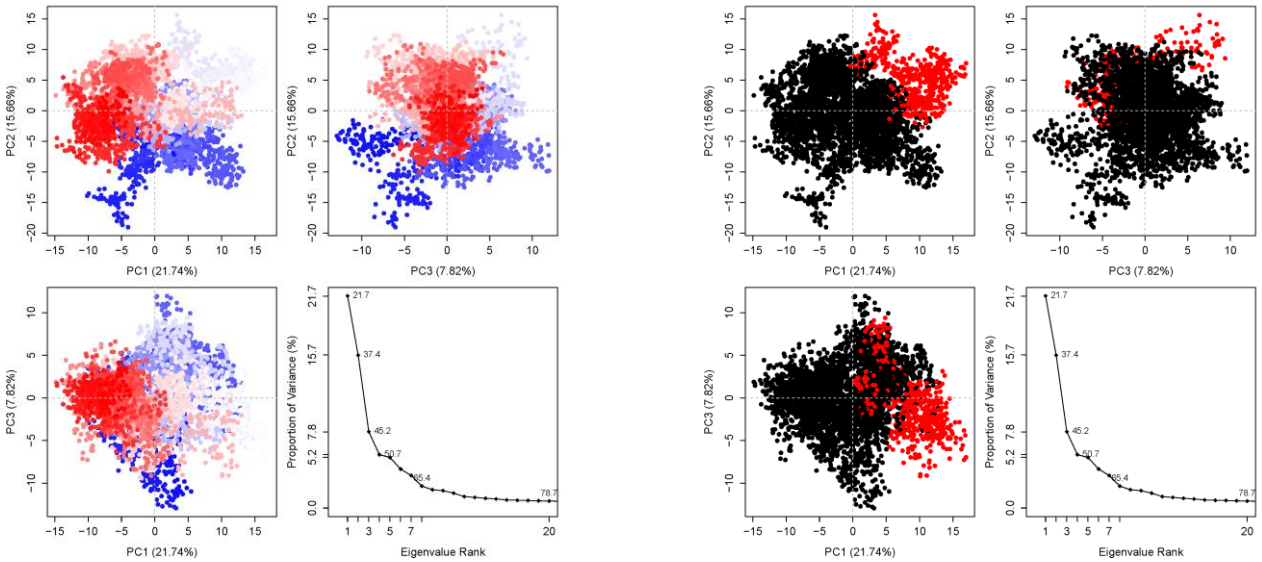

(**a**) (**b**)

Figure S8. (**a**) Principal Component Analysis (PCA) for the MD trajectory of Salmeterol binding into SARS-CoV-2 B.1.351 Variant RBD. The trajectory frames are colored from blue to white to red in time order. (**b**) Simple clustering in PC subspace. The conformations were divided into two clusters (black and red) according to the top 3 PC-spaces shown in the PC subspace.

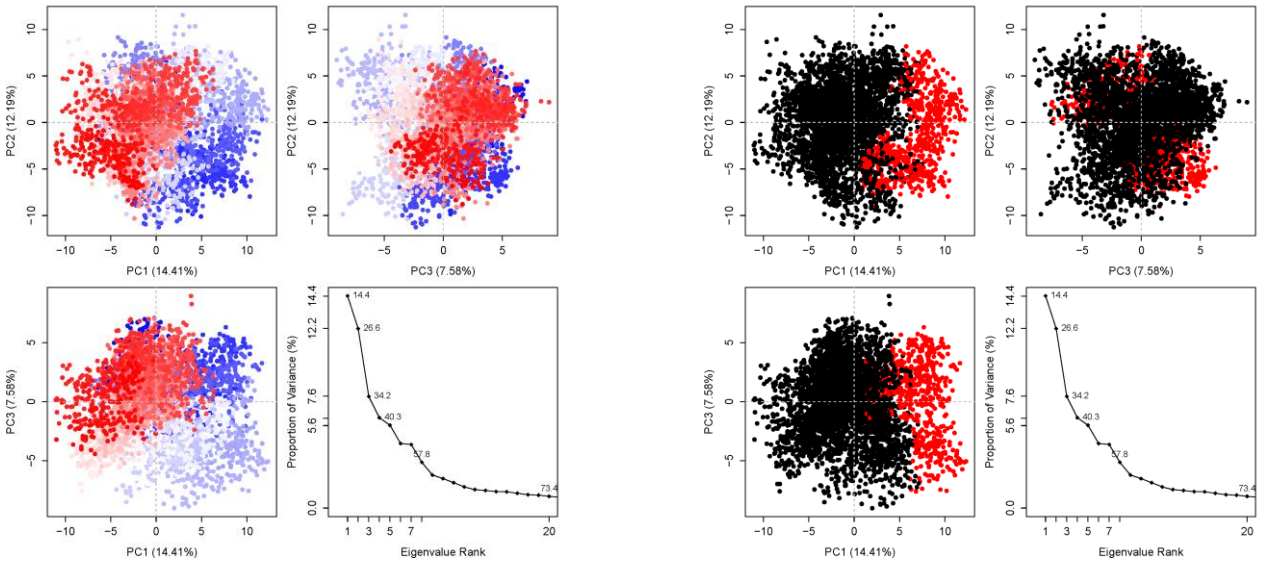

(**a**) (**b**)

Figure S9. (**a**) Principal Component Analysis (PCA) for the MD trajectory of the unbinding process between Salmeterol and SARS-CoV-2 B.1.351 RBD. The trajectory frames are colored from blue to white to red in time order. (**b**) Simple clustering in PC subspace. The conformations were divided into two clusters (black and red) according to the top 3 PC-spaces shown in the PC subspace.

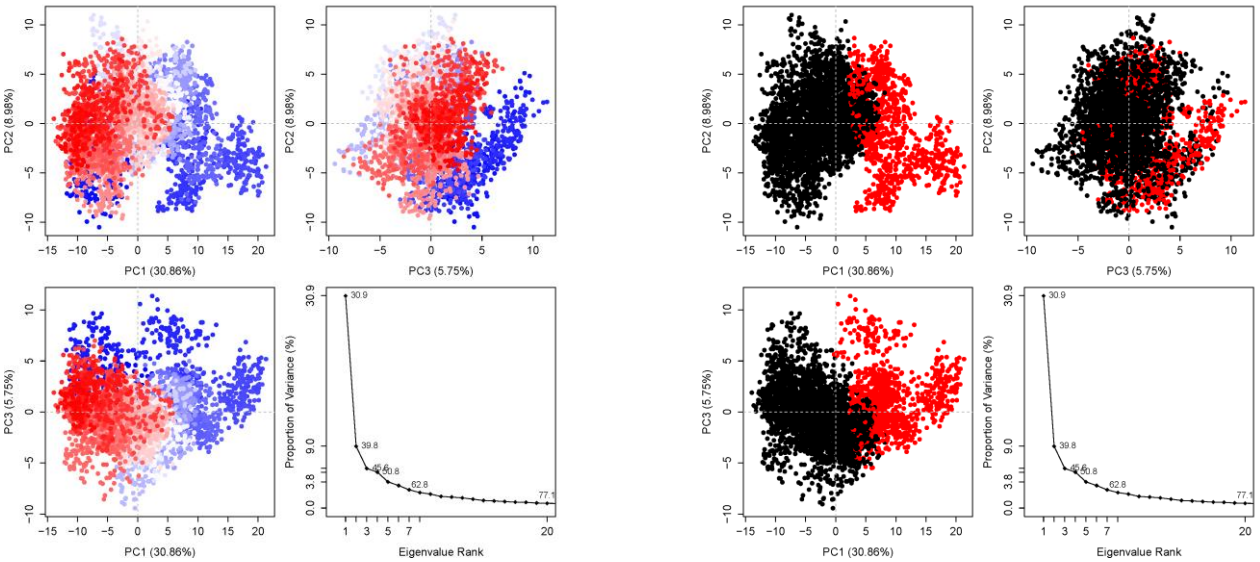

Figure S10. (**a**) Principal Component Analysis (PCA) for the MD trajectory of Salmeterol binding into SARS-CoV-2 P.1 Variant RBD. The trajectory frames are colored from blue to white to red in time order. (**b**) Simple clustering in PC subspace. The conformations were divided into two clusters (black and red) according to the top 3 PC-spaces shown in the PC subspace.

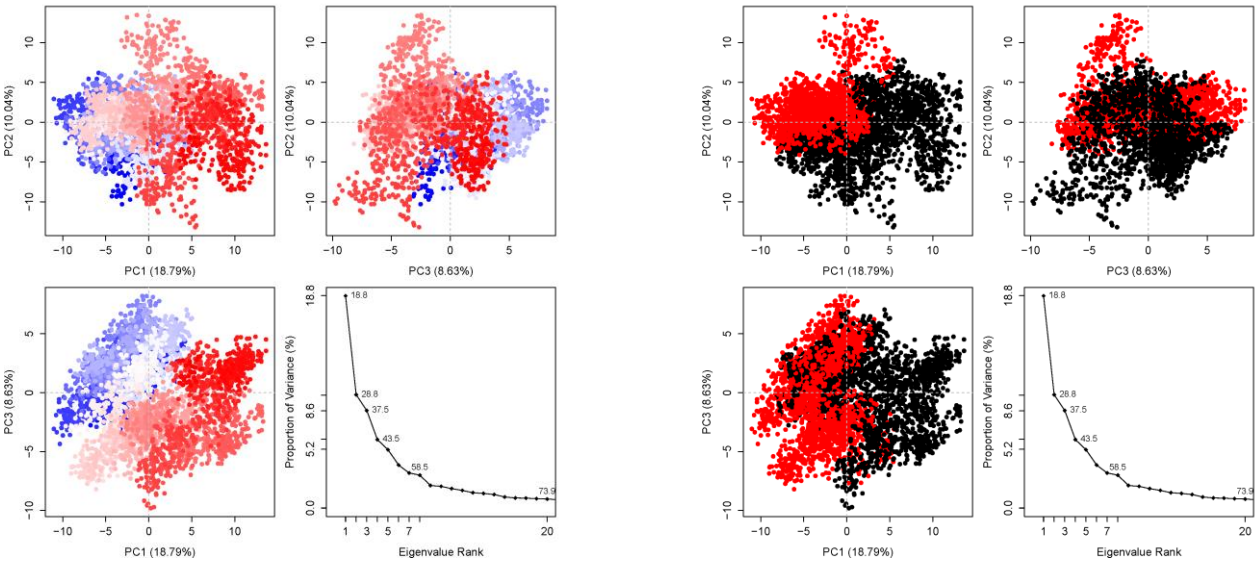

Figure S11. (**a**) Principal Component Analysis (PCA) for the MD trajectory of the unbinding process between Salmeterol and SARS-CoV-2 P.1 RBD. The trajectory frames are colored from blue to white to red in time order. (**b**) Simple clustering in PC subspace. The conformations were divided into two clusters (black and red) according to the top 3 PC-spaces shown in the PC subspace.

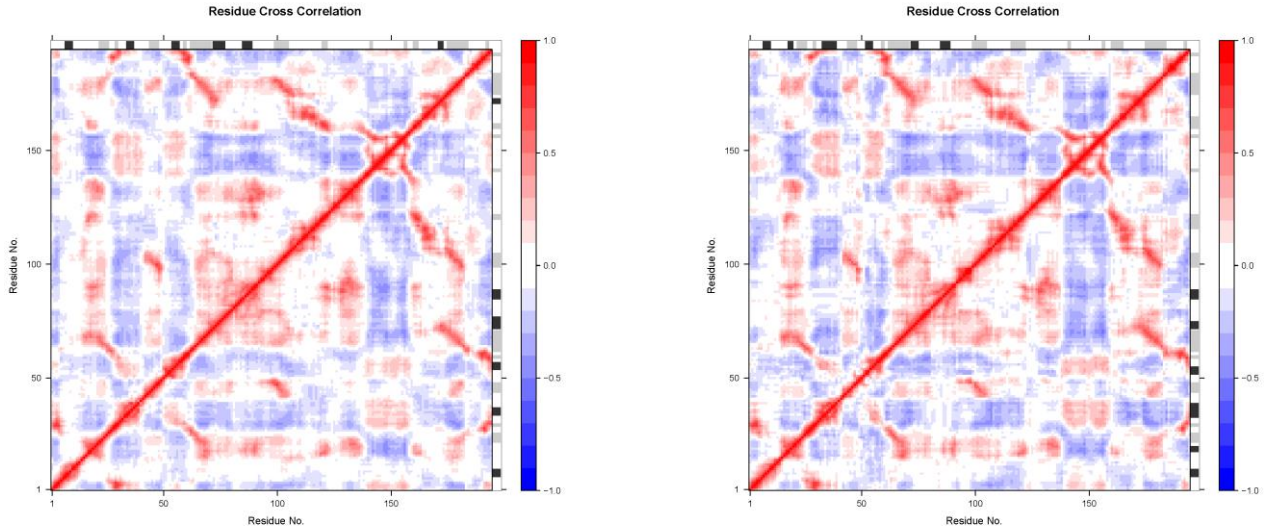

(**a**) (**b**)

Figure S12. Dynamical residue cross-correlation map for the MD trajectory of the (**a**) binding process and (**b**) unbinding process of the receptor-ligand complex involving Salmeterol docked in Wild-type RBD. PCA results for a trajectory with trajectory frames colored from blue to white to red in time order.

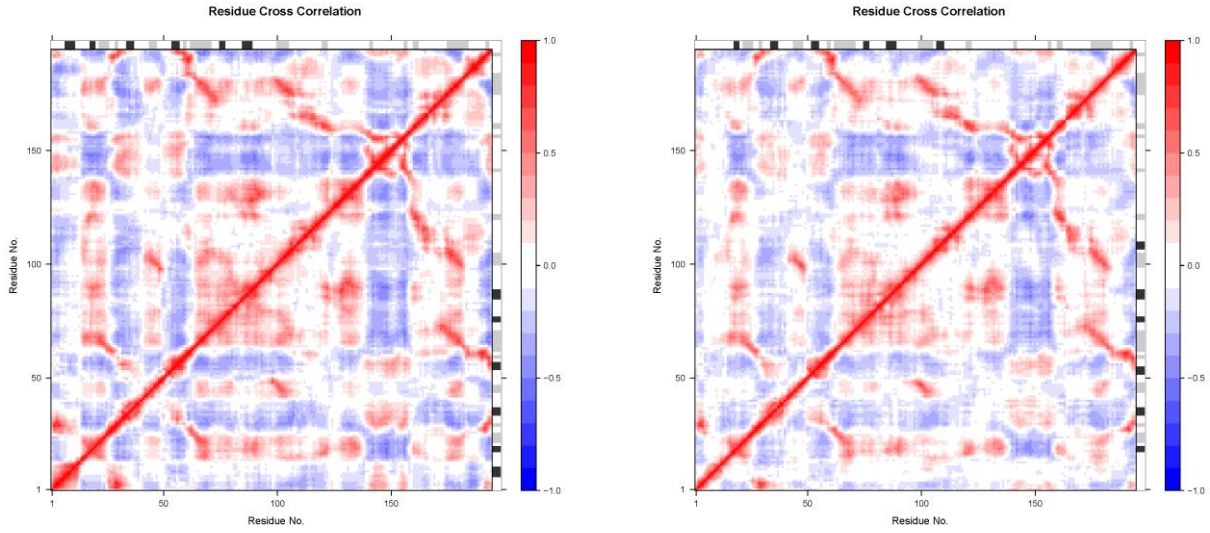

(**a**) (**b**)

Figure S13. Dynamical residue cross-correlation map for the MD trajectory of the (**a**) binding process and (**b**) unbinding process of the receptor-ligand complex involving Salmeterol docked in SARS-CoV-2 B.1.1.7 RBD. PCA results for a trajectory with trajectory frames colored from blue to white to red in time order.

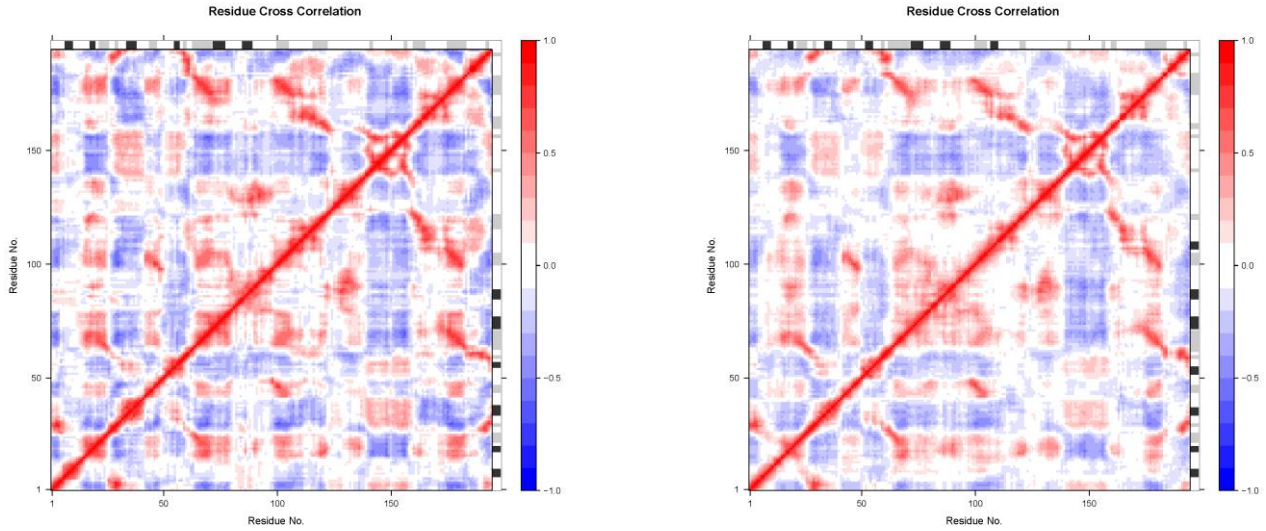

(**a**) (**b**)

Figure S14. Dynamical residue cross-correlation map for the MD trajectory of the (**a**) binding process and (**b**) unbinding process of the receptor-ligand complex involving Salmeterol docked in SARS-CoV-2 B.1.351 RBD. PCA results for a trajectory with trajectory frames colored from blue to white to red in time order.

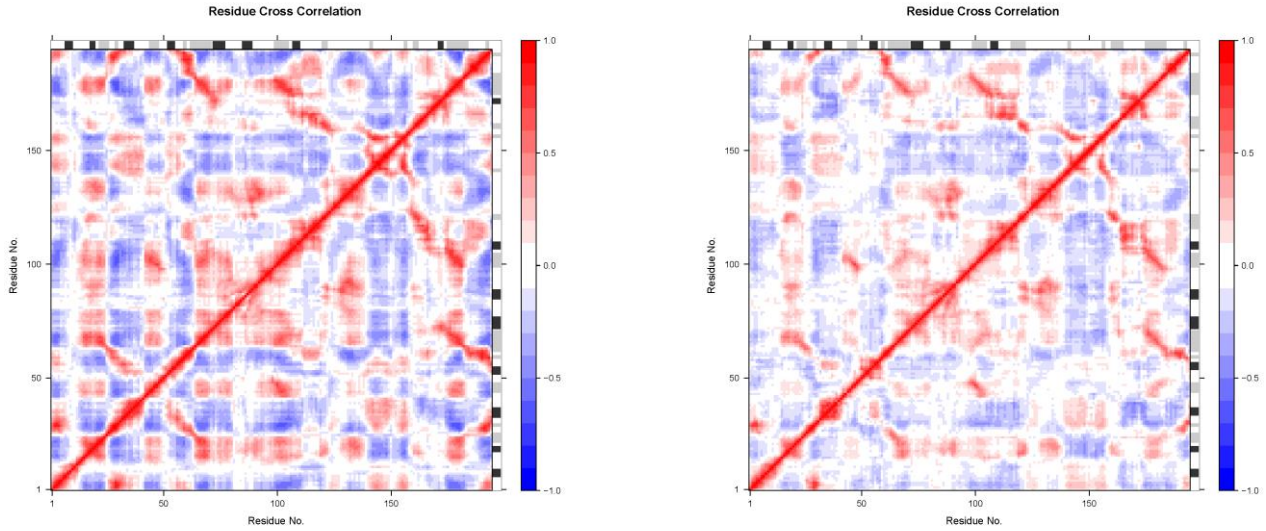

(**a**) (**b**)

Figure S15. Dynamical residue cross-correlation map for the MD trajectory of the (**a**) binding process and (**b**) unbinding process of the receptor-ligand complex involving Salmeterol docked in SARS-CoV-2 P.1 RBD. PCA results for a trajectory with trajectory frames colored from blue to white to red in time order.